JOURNAL OF CATALYSIS **178,** 520–532 (1998)
ARTICLE NO. CA982158

Alkene and Arene Combustion on Pd(111)

Tracy D. Harris* and Robert J. Madix*,†,[1]

*Departments of Chemistry and †Chemical Engineering, Stanford University, Stanford, California 94305-5025

Received November 10, 1997; revised May 15, 1998; accepted May 18, 1998

Oxidation reactions of ethene, propene, 1-butene, 1,3-butadiene, benzene, and toluene were studied on oxygen-precovered Pd(111) (0.25 ML–1.2 ML) using temperature-programmed reaction spectroscopy (TPRS). Combustion is the sole reaction pathway; no partial oxidation products are formed. Comparison of these results with those from Pd(100) demonstrates that the structure of the metal surface does not significantly affect the mechanism of catalytic oxidation of most of the olefins or aromatic hydrocarbons studied, although, in general, combustion occurs at higher temperatures on Pd(111). Only for benzene combustion is there an appreciable structure sensitivity. For all the hydrocarbons studied the CO_2 and CO yields are maximized for an oxygen precoverage of 0.34 oxygen atoms per surface palladium atom. Abrupt increases in carbon oxide production at specific oxygen coverages indicate that oxygen-induced surface reconstructions may play a role in the combustion activity.

1. INTRODUCTION

Palladium-catalyzed combustion reactions can play a significant role in the control of auto emissions in the three-way catalytic converter (1). Platinum-group metals are used to catalyze the oxidation of CO to CO_2 as well as to treat hydrocarbons and NO_x (2). Palladium catalysts have also proven to be active for selective oxidation of hydrocarbons; supported palladium catalysts have been used to selectively oxidize ethene to acetaldehyde (3). In this work we seek to contribute to a fundamental understanding of combustion/oxidation reactions on palladium through an examination of the combustion of alkenes and aromatic hydrocarbons on model Pd(111) surfaces, prepared under ultrahigh vacuum (UHV) conditions.

The oxidation of a number of organic molecules has already been studied on palladium surfaces. Reactive hydrocarbons such as aldehydes, carboxylic acids, alcohols, and ketones react with surface oxygen to form both partial and total oxidation products. For example, oxygen adsorbed on clean Pd(111) reacts with aldehydes to generate carboxylate species in addition to total combustion products (H_2O, CO_2, and CO). At a surface coverage of 0.25 ML ($p(2 \times 2)$-O) oxygen alters the orientation of aldehydes from that on Pd(111), activates polymerization of formaldehyde (although not higher aldehydes), scavenges surface hydrogen atoms, and stabilizes surface carboxylate species (4).

The reactions of several simple carboxylic acids, formic acid, acetic acid, and propanoic acid, on the Pd(111)-(2×2) O surface have also been examined (5). Adsorbed oxygen acts as a Brønsted base to abstract the acidic proton leading to the formation of adsorbed carboxylate and hydroxyl groups. These carboxylates subsequently decompose to CO_2, CO, and H. Water is evolved from recombination of the surface hydroxyl species with H(a).

The interaction of adsorbed oxygen with alcohols on Pd(111) causes oxidation of the alcohols (6). Primary alcohols (methanol, ethanol, 1-propanol) yield primarily the corresponding carboxylate species in addition to the corresponding aldehyde; secondary alcohols (2-propanol) undergo selective oxydehydrogenation to the corresponding ketone. In this case oxidation occurs via a Brønsted acid-base mechanism, whereby the oxygen directly abstracts the acidic hydroxyl proton from the adsorbed alcohol. In these cases, surface oxygen also acts as a nucleophile, attacking adsorbed alcohols to form the observed surface carboxylate species. In addition, the scavenging of excess surface hydrogen by oxygen suppresses any possible hydrogenation reaction of alcohols or surface intermediates.

The reactions of acetylene with oxygen on Pd(111) have been studied for oxygen coverages up to 0.25 ML (7). At lower oxygen coverages (<0.25 ML) both furan (C_4H_4O) and combustion products (H_2O, CO_2, CO) are formed. At 0.25 ML only the combustion products form; furan formation is suppressed. In no cases, however, have the reactions of hydrocarbons been studied at higher oxygen coverages (in excess of 0.25 ML O) on Pd(111). This is an important matter, since much higher surface concentrations of oxygen are known to form on palladium under catalytic oxidizing conditions (8, 9).

The oxidation of alkenes (10) and arenes (11) on Pd(100)-$p(2 \times 2)$-O (0.25 ML O) has also been studied previously. In these studies, total combustion was the only reaction pathway observed; no partial oxidation products were observed. For ethene, which has only terminal sp^2 hydrogens, the adsorbed oxygen inhibits reaction, and only a small amount of adsorbed oxygen reacts. However, surface oxygen *activates* combustion reactions of propene, 1-butene, and

0021-9517/98 $25.00

1,3-butadiene, which possess both allylic and vinylic hydrogens. Combustion products are evolved below the temperatures at which dehydrogenation of the alkenes occurs on clean Pd(100). Furthermore, total combustion is the only reaction detected at oxygen precoverages up to 1 ML. The adsorbed intermediates involved in oxidation of aromatic hydrocarbons (benzene, toluene, and styrene) on Pd(100)-$p(2 \times 2)$-O are *directly* attacked and destabilized by O(a). The reactivity of the aromatic molecules with adsorbed oxygen decreases from toluene to styrene to benzene, paralleling the trend in their gas phase acidities. The aromatic hydrocarbons were not examined at higher surface oxygen coverages.

In this work we have examined the reactions of ethene, propene, 1-butene, 1,3-butadiene, benzene, and toluene on 0.25 ML O on Pd(111) (the saturation coverage reached with dioxygen dosing (12)); combustion is the sole reaction observed for these systems. Because no partial oxidation products were generated (as they were not on Pd(100)), it can be concluded that the metal surface structure has little effect on the overall oxidation mechanism of olefins and aromatics on palladium. Also examined was the role of increasing surface oxide coverage (up to 1.2 ML oxide O/NO_2) on the combustion product yields and reaction mechanism for three representative molecules: ethene, propene, and benzene. The combustion yields for these three hydrocarbons are strongly dependent on surface oxygen coverage above 0.25 ML.

2. EXPERIMENTAL

All experiments were performed in a stainless steel UHV chamber with a base pressure of 4×10^{-10} torr. The Pd(111) crystal was prepared using standard metallographic techniques. The crystal was cleaned initially with argon ion sputtering at 300 K and annealing to 1000 K to remove sulfur impurities. Carbon impurities were removed via repetitive cycles of oxygen dosing (1000 K) followed by annealing to 1100 K. Low energy electron diffraction (LEED) revealed a well-ordered (111) surface. To verify that the palladium surface was free from carbon contaminants, temperature programmed desorption (TPD) after subsequent oxygen exposure was utilized; the surface was deemed free of carbon when no CO_2 and/or CO desorption was observed. Auger electron spectroscopy (AES) was used to verify the absence of other surface contaminants, such as sulfur. The crystal was routinely cleaned by oxygen dosing followed by annealing to 1100 K. The crystal was heated via resistive heating and was cooled to temperatures below 100 K with the use of a liquid nitrogen reservoir. Temperature was monitored by a chromel-alumel thermocouple spot welded to the back of the crystal.

Reactants were dosed onto the crystal via stainless steel capillary array dosers positioned less than 4 mm away from the surface. High-purity alkenes (ethene, propene, 1-butene, 1,3-butadiene), oxygen, and nitrogen dioxide were used directly from lecture bottles (Matheson) without further purification. C_2D_4 (99% purity) and $^{18}O_2$ (98% purity) were obtained from Cambridge Isotope Laboratories and were also used directly from the lecture bottles without further purification. Liquid aromatics (benzene, toluene) (Aldrich, 99+% purity) were purified by multiple freeze-pump-thaw cycles each day before use. Methyl-d_3 toluene (85% $C_6H_5CD_3$, Cambridge Isotope Laboratories) was similarly purified. Utilizing TPD areas, surface oxygen coverages were calibrated with respect to the 0.25 ML (p-2×2) saturation coverage of oxygen on Pd(111) dosed at 300 K (12). Higher oxygen coverages (up to ~1.2 ML) were achieved by dosing varying amounts of NO_2 at 530 K (8). The crystal was cooled to less than 100 K (typically 95 K) for hydrocarbon dosing.

Temperature programmed reaction spectra (TPRS) data were monitored by a UTI 100C quadrupole mass spectrometer interfaced to an IBM XT computer; this setup allows multiplexing of up to 150 masses. However, during most TPRS experiments, in order to achieve a better signal-to-noise ratio, no more than 10 masses were monitored simultaneously. A glass cap with a 3-mm aperture was affixed to the mass spectrometer ionization grid, ensuring that only molecules desorbing from the center of the single crystal surface were admitted to the mass spectrometer ionizer during TPRS. Before each experiment the crystal was cooled to a temperature of 100 K. The crystal was then heated approximately linearly at a rate of ~18 K/s. The amount of background adsorption of H_2, CO, and CO_2 from the chamber was calibrated from blank TPRS experiments (T = 100 K, no hydrocarbon exposure). To provide a basis for understanding the mechanisms of combustion product formation, the TPRS data were compared to "standard" spectra we obtained for H_2, H_2O, CO, and CO_2 formed from recombination or desorption of surface species (e.g., $2H(a) \rightarrow H_2(g)$ designated as $H_2/H + H$, $CO(a) \rightarrow CO(g)$ designated as CO/CO or $C(a) + O(a) \rightarrow CO(g)$ designated as CO/C + O) (Fig. 1). Of note is the fact that on clean Pd(111), CO_2 has a desorption temperature below that which we could achieve (13, 14). Any CO_2 observed to desorb in the oxidation reactions must be rate-limited by a surface reaction.

Yields of H_2 were calibrated by comparison of TPD areas to the saturation coverage ($\theta = 1$ ML) (15) of H_2 on Pd(111). CO yields were calibrated to the saturation coverage ($\theta =$ 0.66 ML) at 200 K (16). Yields of CO_2 were obtained using the mass spectrometer sensitivity calibration relative to CO (17). The Redhead equation (18)

$$\frac{E}{RT_p^2} = \frac{\nu_1}{\beta} \exp\left(\frac{E}{RT_p}\right) \qquad [1]$$

was used to estimate desorption and activation energies

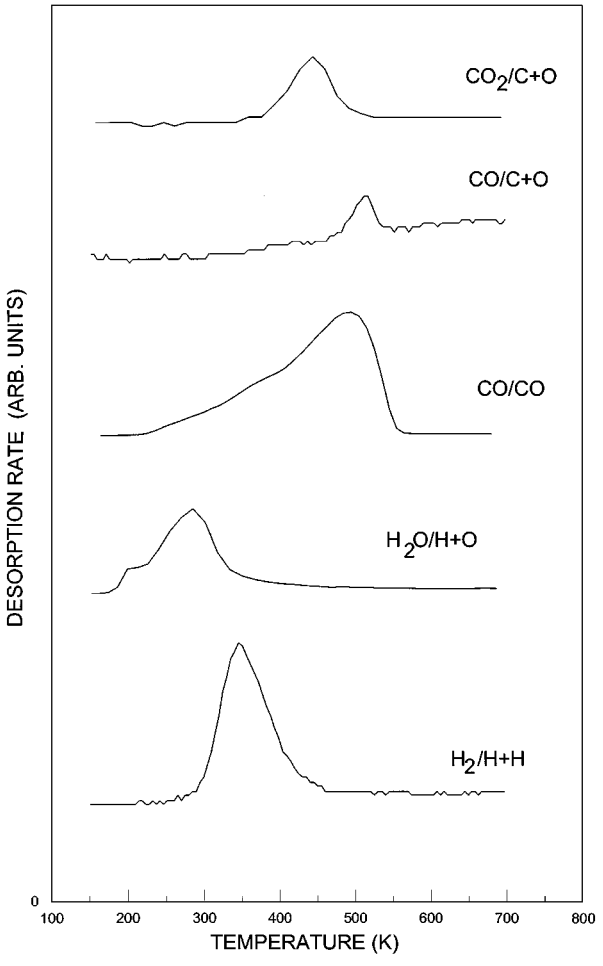

FIG. 1. The evolution of product molecules H_2, H_2O, CO, and CO_2 from Pd(111) and Pd(111)-$p(2 \times 2)$-O.

(E, kcal/mol) from the TPRS peak temperatures (T_p, K), assuming both a first-order reaction and a preexponential factor (ν_1) of 10^{13} s^{-1}. The TPR spectra most concisely and completely show the complexities of the oxidation reactions. On inspection they indicate changes in activation energies by shifts in peak temperatures and the relative importance of different reaction channels (by different peak intensities at the different peak temperatures) with changing conditions. Because any attempt at a tabular representation of this information would be hopelessly complex, the TPR spectra are presented in their entirety.

3. RESULTS

3.1. Ethene

The combustion of ethene (C_2H_4) on Pd(111) differs from that of the other hydrocarbons studied in this work in that the ethene is much less reactive on the oxide surface than the other hydrocarbons. With an oxygen precoverage of 0.25 ML (Fig. 2) most of the ethene desorbs molecularly, peaking at 280 K; desorption, is complete by 400 K. The only mass peak attributed to H_2 is a tiny peak (not observable on the scale utilized to characterize the reaction products) coincident with the 280 K ethene desorption, which is attributed to a cracking fraction of ethene. Small yields of H_2O and CO_2 are generated from combustion. Water formation commences at 160 K as ethene desorbs, peaking at 175 and 290 K, and trailing off near 425 K. Next, a small amount of CO_2 is produced between 350–580 K. Finally, excess oxygen (~0.24 ML) desorbs in a broad feature which peaks ~790 K. This oxygen excess ensures that no C(a) residue remains. Because ethene was so unreactive on the oxygen-covered surface, the effects of higher oxygen coverages were tested.

The ethene desorption features change with surface oxygen coverage, as shown in Fig. 3a. Between oxygen coverages of 0.25 and 0.34 ML ethene desorption peaks near 290 K, but as the initial oxygen coverage is increased to 0.71 ML, the desorption peak temperature decreases to 225 K. With a further increase in oxygen coverage to 1.2 ML, the desorption features change greatly; new ethene desorption features are seen at 160 K, 245 K, and 280 K. The ratios

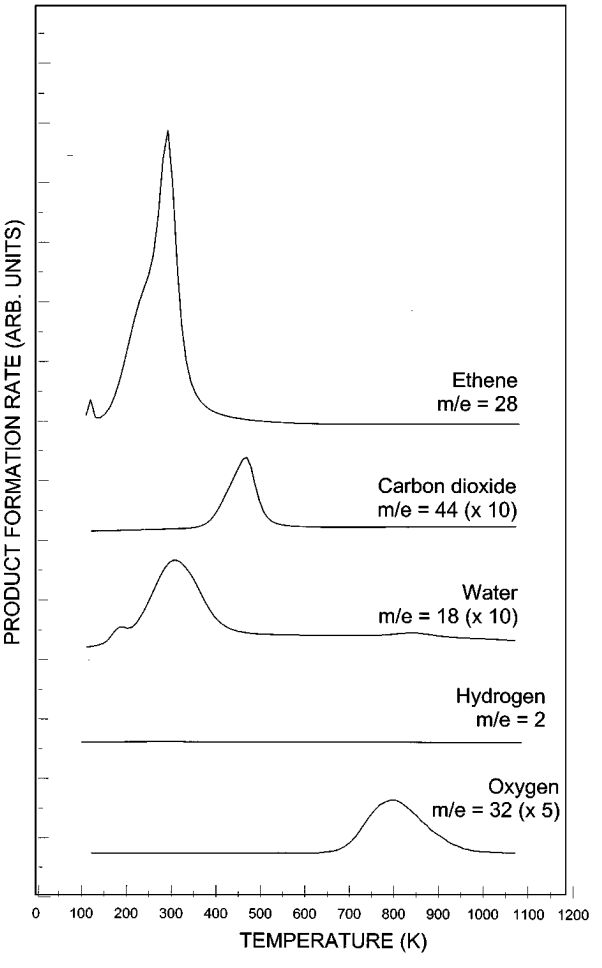

FIG. 2. TPRS spectra of ethene adsorbed on Pd(111)-$p(2 \times 2)$-O.

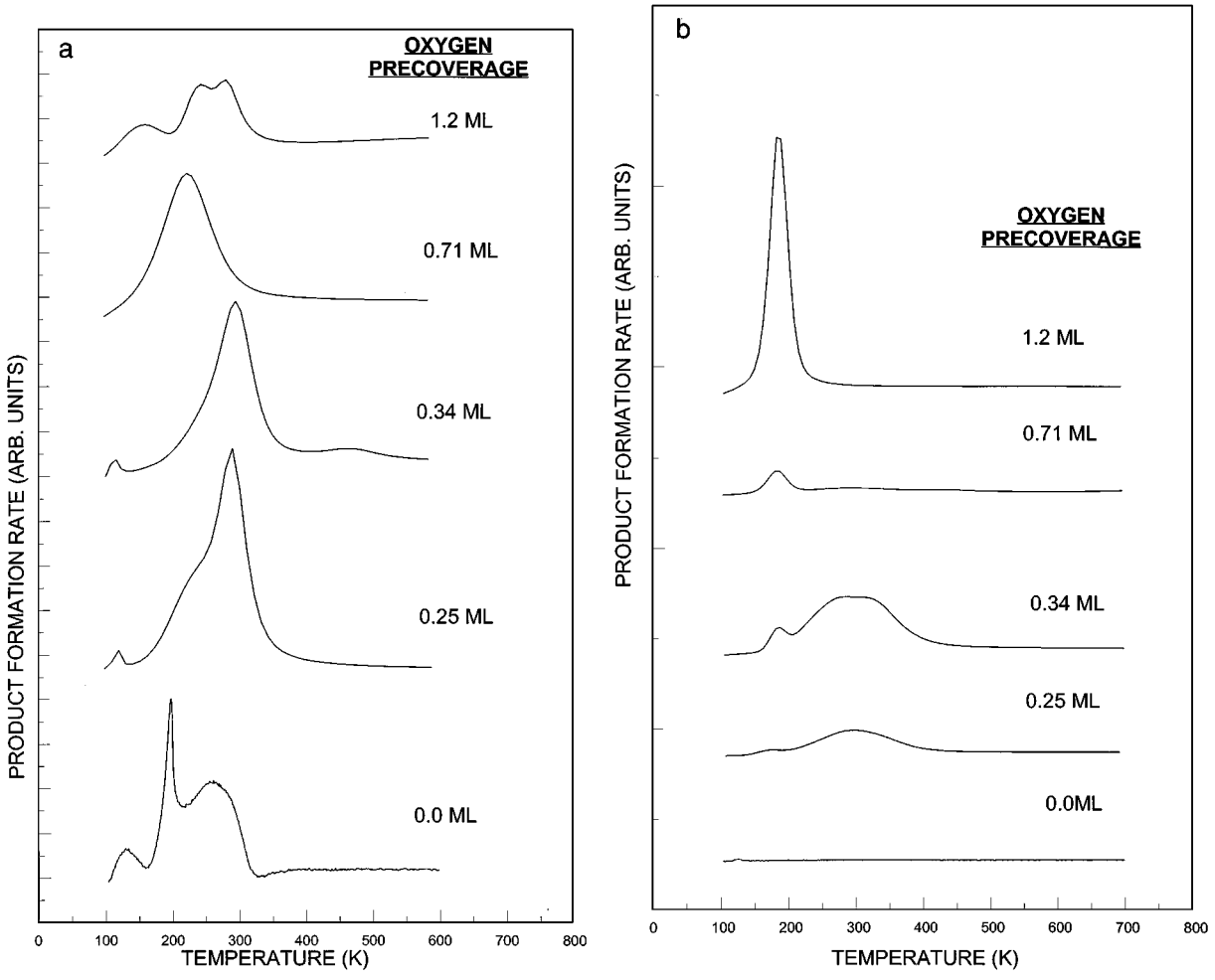

FIG. 3. TPRS spectra following ethene adsorption on Pd(111)-O at varying levels of oxygen precoverage: (a) ethene; (b) H_2O.

of the amounts of desorbing ethene for 0.25 ML O : 0.34 ML O : 0.71 ML O : 1.2 ML O are 1 : 0.69 : 0.77 : 0.55. In contrast, on the clean Pd(111) surface, molecular ethene desorption commences at ∼175 K, peaks at 200 K, and continues to 320 K. Furthermore, on the clean surface ethene dehydrogenates, significantly reducing the proportion of ethene which desorbs intact. Since adsorbed hydrogen atoms react so readily with adsorbed oxygen, it is unlikely that the ethene desorption on the oxygen precovered surfaces arises from the reductive elimination of partially dehydrogenated fragments. It thus appears that the binding energy of ethene to the surface at oxygen precoverages of 0.25 and 0.34 ML is approximately 18 kcal/mol, being reduced to 14 kcal/mol at a coverage of 0.71 ML. The reemergence of higher temperature binding states for ethene at 1.2 ML suggests that the surface undergoes structural changes between 0.71 and 1.2 ML oxygen coverage.

At intermediate oxygen coverages ($\theta = 0.25$, 0.34 ML) the kinetics of water evolution resembles that typical of the reaction between coadsorbed hydrogen and oxygen (Figs. 1 and 3b). As oxygen coverage is increased from 0.25 to 0.34 ML the H_2O yield increases (Table 1). At 0.71 ML O, the higher temperature peak has disappeared, leaving only a single small peak at 180 K. At 1.2 ML O the 180 K peak has increased almost fivefold. Two notable features emerge from these experiments. First, there is a marked reduction in reactivity at an oxygen coverage of 0.71 ML; second, the dominant pathway for water formation at the highest oxygen coverage occurs at 180 K. The latter result may be due either to a reduction in the characteristic reaction temperature for the H + O reaction or due to the direct attack of adsorbed ethene by adsorbed oxygen.

TABLE 1

Water Yield as a Function of Surface Oxygen Coverage (Vs)

	0.0 ML O	0.25 ML O	0.34 ML O	0.59 ML O	0.71 ML O	1.2 ML O
Ethene	0	0.98	2.5	N/A	0.39	2.6
Propene	0	7.7	5.3	N/A	3.4	3.3
Benzene	0	2.5	1.2	0.37	0.18	0.99

Carbon dioxide is formed by oxygen scavenging of carbonaceous residues near 450 K at all initial oxygen coverages (spectra not shown). The CO_2 yield increases fourfold between oxygen precoverages of 0.25 and 0.34 ML, but decreases sharply as the coverage is increased to 0.71 ML. At 1.2 ML O the CO_2 evolves in reaction-limited peaks at 400 K and 500 K; the yield also increases slightly above that observed at 0.71 ML O coverage. At all oxygen coverages studied excess oxygen desorbs at ~775 K–800 K (800 K for lower initial oxygen exposures, 775 K for higher). No CO production is observed, which is to be expected, as surface oxygen is in excess of accessible carbon. However, very small amounts of $m/e = 28$ which coincide exactly with CO_2 evolution are observed; these are attributed to CO^+ cracking fractions of CO_2. The observed intensity ratios agree well with the literature mass spectral ratio of $CO_2 : CO^+$ of 100 : 8 (19). As was true for 0.25 ML O, because of the surface oxygen excess, no $C_{(a)}$ is observed. No other products were found.

To verify that no partial oxidation products were formed, isotopic experiments were performed. Experiments with deuterated ethene (C_2D_4) on O/Pd(111) and experiments with C_2H_4 on ^{18}O/Pd(111) confirmed that only total combustion products, H_2, and C(a) are formed during ethene combustion of Pd(111). A kinetic isotopic effect on the reactivity was apparent with C_2D_4, as reaction yields were even smaller than those seen with C_2H_4.

3.2. Propene, 1-Butene, 1,3-Butadiene

The reaction of propene on a 0.25-ML oxygen-covered Pd(111) surface yields combustion products (H_2O, CO_2, CO) as well as $C_{(a)}$ and small amounts of H_2 (Fig. 4). In contrast to ethene, all the oxygen is consumed in the combustion reaction. Propene itself desorbs in several states between 100 and 420 K; desorption maxima are observed at 155 and 205 K, followed by a smaller peak near 295 K and a final state at 390 K. Water formation begins at 200 K, exhibits one rate maximum at 305 K which is followed by a larger peak at 400 K (coinciding with the end of propene evolution) which tails to 500 K. As the H_2O production at 400 K decreases, a small amount of H_2 desorbs, with a peak at 420 K followed by a broad feature which ends above 800 K. CO_2 and CO peaks evolve coincident with the 400 K H_2O desorption feature; CO desorbs in a second, large peak at 520 K. The evolution of H_2 is indicative of the consumption of the initially adsorbed oxygen.

The complexity of molecular propene desorption on the oxide surface at higher oxygen precoverages suggests multiple bonding configurations and/or surface interactions (Fig. 5a). As the oxygen precoverage is increased from 0.25 to 0.34 ML, the desorption peak at 390 K disappears, and propene peaks are seen at 120 K and 230 K, with a shoulder at 295 K. As the coverage is increased further, this shoulder increases in size, while the peak at 230 K decreases.

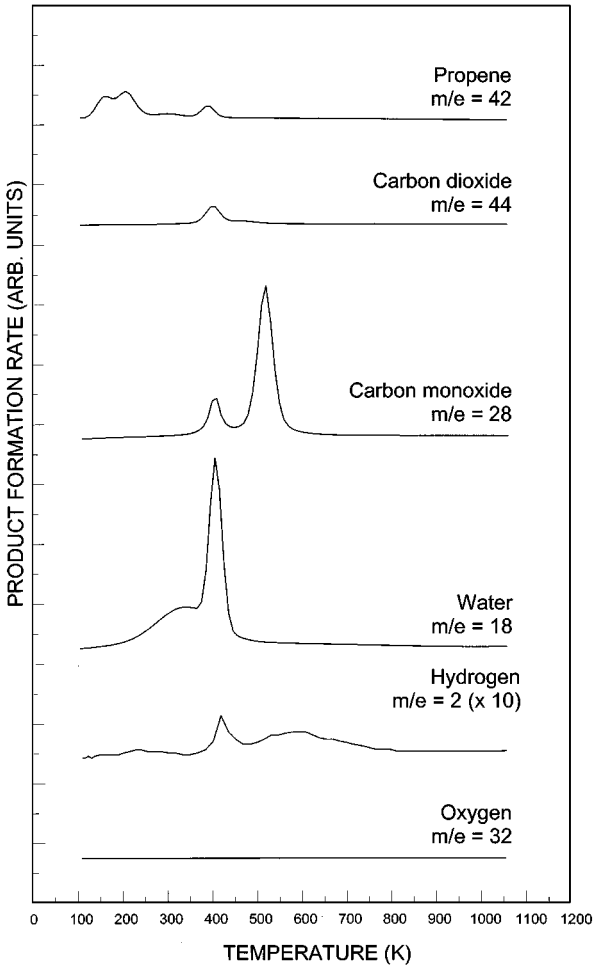

FIG. 4. TPRS spectra of propene adsorbed on Pd(111)-$p(2 \times 2)$-O.

At 1.2 ML oxygen, propene exhibits major peaks at both 130 K and 295 K, the latter being preceded by a shoulder at 265 K. Of note is the fact that as the oxygen coverage is increased above 0.34 ML, there is not a significant change in the *amount* of propene desorbing, rather it just shifts preferentially to the state that desorbs at the higher temperature (295 K). In contrast, on clean Pd(111) propene desorbs molecularly as follows: a sharp peak centered at 190 K, followed by a broad, smaller peak at 275 K which extends to 400 K; desorption competes with decomposition on the clean surface, of course.

The temperature of formation (Fig. 5b) and yields (Table 1) of water from propene combustion are affected by surface oxygen coverage. As the oxygen precoverage increases, the water yield decreases. As noted above, at 0.25 ML O, H_2O desorption begins near 200 K and exhibits maxima in rate at 305 K and 400 K (coinciding with the end of propene evolution). At 0.34 ML oxygen some water evolution commences at 140 K, suggesting that oxygen directly abstracts hydrogen from the hydrocarbon well below room temperature. The dominant routes to H_2O seen at 300 and

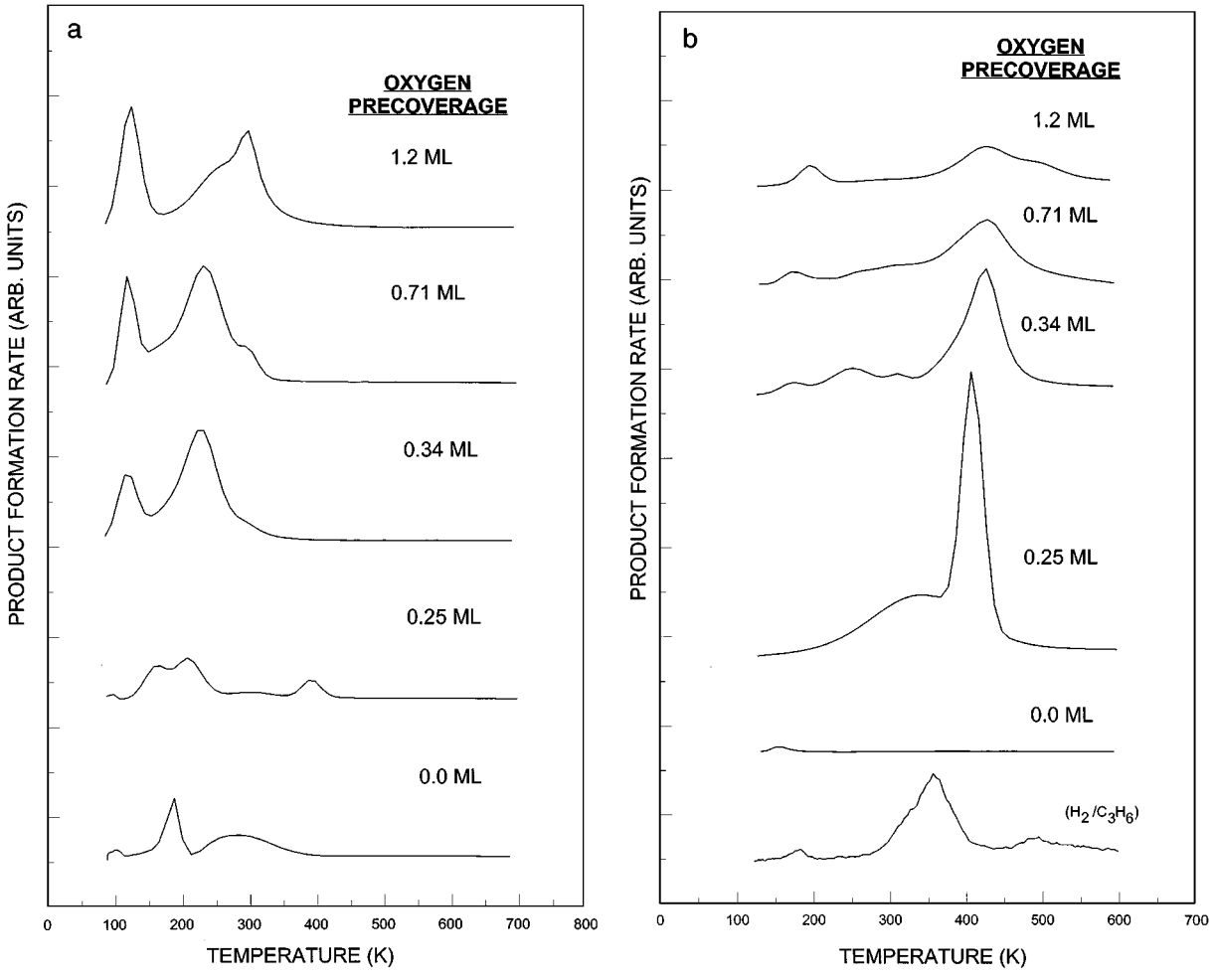

FIG. 5. TPRS spectra following propene adsorption on Pd(111)-O at varying oxygen precoverages: (a) propene; (b) H_2O (bottom trace is H_2 evolution from the propylene adsorbed on the clean surface, reproduced from (20)); (c) CO_2; (d) CO.

420 K are similar to the features on the 0.25 ML surface; however, as the oxygen precoverage reaches 1.2 ML, there is a small water peak at 200 K followed by the peak at 420 K with a shoulder at 485 K. On the clean surface propene dehydrogenation is seen in two stages; desorption-limited hydrogen evolves at 361 K followed by a broad reaction-limited peak (18). The fact that a significant portion of the water evolution occurs at or above the temperatures for dehydrogenation on the clean surface indicates that dehydrogenation followed by oxygen attack and/or scavenging may account for a significant portion of the combustion at all oxygen coverages.

The evolution of carbon dioxide during propene combustion parallels the peaks for water (Fig. 5c). Aside from the low temperature peaks for water formation, carbon dioxide and water are evolved at the same temperatures, indicative of common rate-limiting steps in their formation. At an oxygen coverage of 0.34 ML, CO_2 production increases dramatically above that observed at 0.25 ML, the peak at 405 K observed at 0.25 ML O becoming a shoulder on a larger peak near 455 K. A higher temperature route seems to turn on at this coverage. As the oxygen coverage is increased further, the CO_2 yield begins to decrease. At 1.2 ML the peak positions change, with a peak at observed at ~430 K followed by a shoulder at 505 K.

At an oxygen precoverage of 0.25 ML CO evolves in two sharp peaks; the first at 405 K and the second, larger peak at 520 K (Fig. 5d). On Pd(111) molecularly adsorbed CO desorbs around 490 K, whereas recombination reaction-limited CO appears at ~535 K (21); hence, the low CO peak temperatures found in this system cannot be assigned to recombination of adsorbed carbon and oxygen atoms to form CO; it is most likely formed by direct oxygen attack on adsorbed propene, with the binding energy of the molecular CO lowered by lateral interaction with adsorbed molecular fragments. As the oxygen coverage is increased, the dominant pathway shifts to lower temperature routes; at 0.34 ML O, a large CO peak at 450 K is preceded by a shoulder at 405 K and followed by a small peak at 530 K. At 0.71 ML oxygen only a small peak at 450 K is seen while at 1.2 ML O

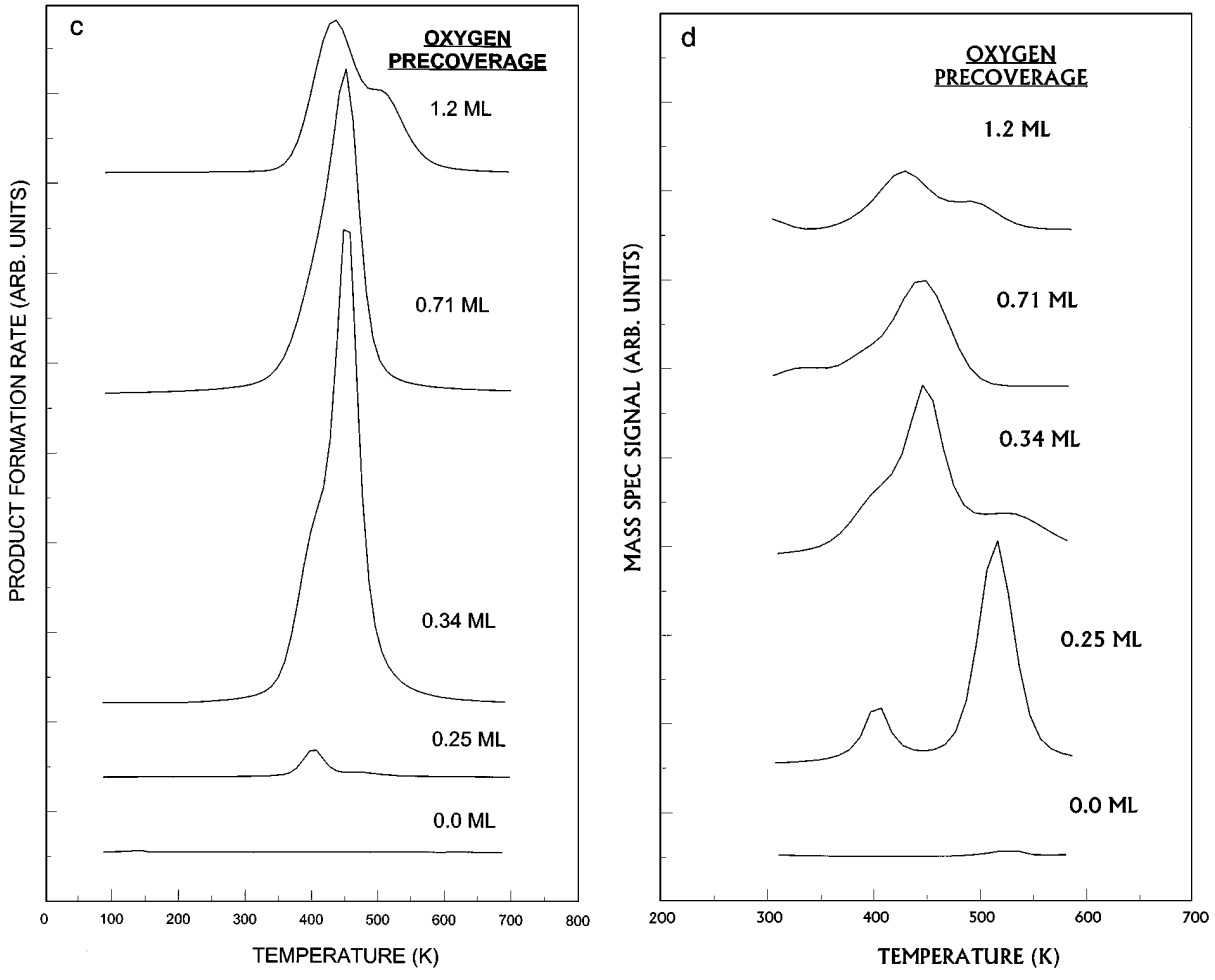

FIG. 5—*Continued*

two CO peaks are seen at 420 K and 500 K. (The CO peaks at 340 and 290 K, respectively, are attributed to cracking fractions of CO_2 desorbing from the sample holder.) The peaks observed at temperatures below 490 K cannot be attributed to cracking fractions of CO_2, which evolves simultaneously, since the relatively large yield at $m/e = 28$ exceeds the expected mass spectral ratio of CO^+ to CO_2 ($\sim$8%) [17]. The temperature at which combustion products begin to appear corresponds closely to the dehydrogenation temperature of propene on Pd(111) on the clean surface (390 K), suggesting that oxidation of hydrocarbon fragments may be triggered by the initial dehydrogenation step. However, we cannot conclude this as oxygen may alter the activation energy for dehydrogenation also. For surface oxygen coverages of 0.34 ML or larger no residual C(a) is seen, due to the presence of an oxygen excess. The small water peaks for 0.34, 0.7, and 1.2 ML oxygen are suggested that defects in the surface structure may contribute to the combustion pathway.

Aside from very minor differences the reactions of 1-butene and 1,3-butadiene on a 0.25 ML oxygen-covered Pd(111) surface are identical to that of propene, as evidenced by their TPRS. The reactions yield combustion products (H_2O, CO_2, CO) as well as C(a) and small amounts of H_2 at temperatures corresponding to those seen in propene combustion. No partial oxidation products are observed. No oxygen desorption is observed; hence all the oxygen is used in the combustion reaction. The parent molecule desorbs first, followed by H_2O evolution, then CO_2 and CO. As the H_2O peak decreases, H_2 begins to evolve, as shown in Fig. 4 for propene. C(a) remains after the reaction has run to completion because the accessible alkene is in stoichiometric excess of surface oxygen.

3.3. Benzene, Toluene

When dosed to achieve coverages greater than a monolayer on the $p(2 \times 2)$-O surface, benzene desorption first occurs from a multilayer state at 94 K (Fig. 6). Molecular benzene then desorbs from the monolayer in smaller peaks at 145 K, 190 K, 280 K, and 415 K. Reaction with oxygen yields combustion products (H_2O, CO_2, CO) and,

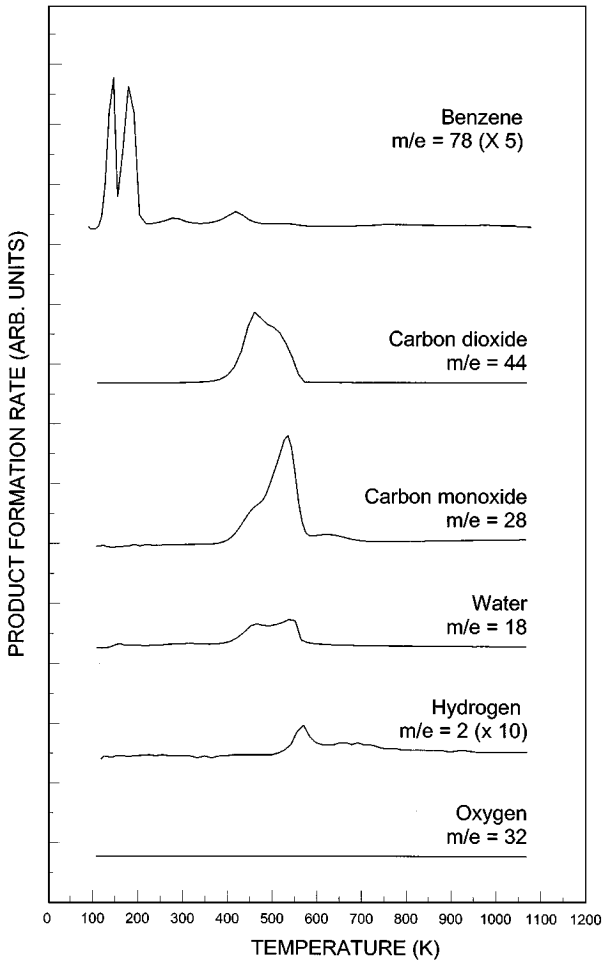

FIG. 6. TPRS spectra of benzene adsorbed on Pd(111)-$p(2 \times 2)$-O.

in addition, H_2 and C(a). Because no oxygen desorption is observed, it is apparent that all the preadsorbed oxygen is consumed in the combustion reaction. Combustion products first evolve at 390 K, with concurrent evolution of CO_2, CO in peaks at 455 K, and H_2O at 465 K. A second set of combustion peaks in which the relative amounts of CO_2 and CO are inverted occurs just above 500 K. At the end of water evolution a small amount of H_2 desorbs, with a small peak at ~575 K followed by a broad feature from 600–790 K. The onset of hydrogen evolution has been associated with the consumption of oxygen in previous work (11). The desorption of benzene is affected significantly when the oxygen coverage is increased above 0.25 ML (Fig. 7a). Most significantly, the area of the 190 K peak decreases, and the features above 400 K disappear, being replaced by a broad, large desorption feature near 300 K. This behavior parallels that noted for propene.

The progression of desorption states for benzene differs from that observed on the clean surface where at high coverages the desorption of benzene occurs at 158 K from a state in which the benzene ring is tilted with respect to the crystal surface (22), followed by two peaks at 400 and 500 K resulting from the desorption of benzene oriented parallel to the surface (23). The presence of oxygen significantly lowers the low coverage binding energy of benzene.

The combustion of benzene begins at temperatures higher than that observed for the alkenes at all oxygen coverages. The onset of water evolution from benzene combustion occurs near 400 K at oxygen coverages of 0.25 and 0.34 ML, nearly 150 K higher in temperature than the alkenes (Fig. 7b). The relative amount of water formed is significantly less than that observed for propene (Table 1). As oxygen coverage increases to 0.34 ML the rate of H_2O evolution peaks at 500 K in a single sharp feature (Fig. 7b); however, the net H_2O yield decreases. At 0.59 and 0.71 ML O very little combustion occurs, and the 500 K peak shifts to 515 K. At 1.2 ML O a number of new reaction channels appear at lower temperature. Although the surface remains reactive toward benzene at the highest oxygen coverage, its reactivity clearly is diminished.

Carbon dioxide and carbon monoxide are evolved simultaneously with nearly identical peak temperatures and peak shapes (Fig. 7c, CO spectra not shown). On the $p(2 \times 2)$-O surface, CO_2 evolution begins at 400 K, reaches maxima at 455 and 505 K, and then tails to 585 K. At 0.34 ML O the lower temperature CO_2 and CO exhibit a single sharp desorption peak at 515 K. As the oxygen precoverage reaches 1.2 ML the peak temperature rises to 550 K. This high peak temperature suggests that the hydrocarbon intermediate which yields the carbon dioxide is stabilized by increasing surface oxygen coverage. At surface oxygen coverages of or exceeding 0.34 ML no C(a) is seen due to the oxygen excess.

Toluene combustion was studied only on the 0.25 ML oxygen-covered Pd(111) surface (Fig. 8). Like benzene, the reaction yielded the expected combustion products, as well as C(a) and small amounts of H_2, which evolves when the preadsorbed oxygen is consumed. No partial oxidation products were observed, and all the oxygen was consumed. The toluene multilayer desorbs at 90 K (data not shown). Molecular toluene desorption peaks sharply at 145 K and is followed by a smaller peak at 195 K and a still smaller feature at 255 K; desorption is complete by 300 K.

Combustion commences at a much lower temperature than seen for benzene; water evolution begins near 250 K. However, the evolution of the carbon oxides is not complete until 550 K, exactly as found for benzene. The water evolution at the lower temperature (320 K) is due to the reactivity of the methyl hydrogens, as shown by selective labeling with methyl-D toluene ($C_6H_5CD_3$, 85%), while the high temperature water yield is the result of reactions of the phenyl group. The methyl hydrogen atoms are clearly more reactive with the oxygen-covered Pd(111) surface than the aromatic hydrogen atoms. CO_2 evolution commences at 375 K and peaks at 455 K;

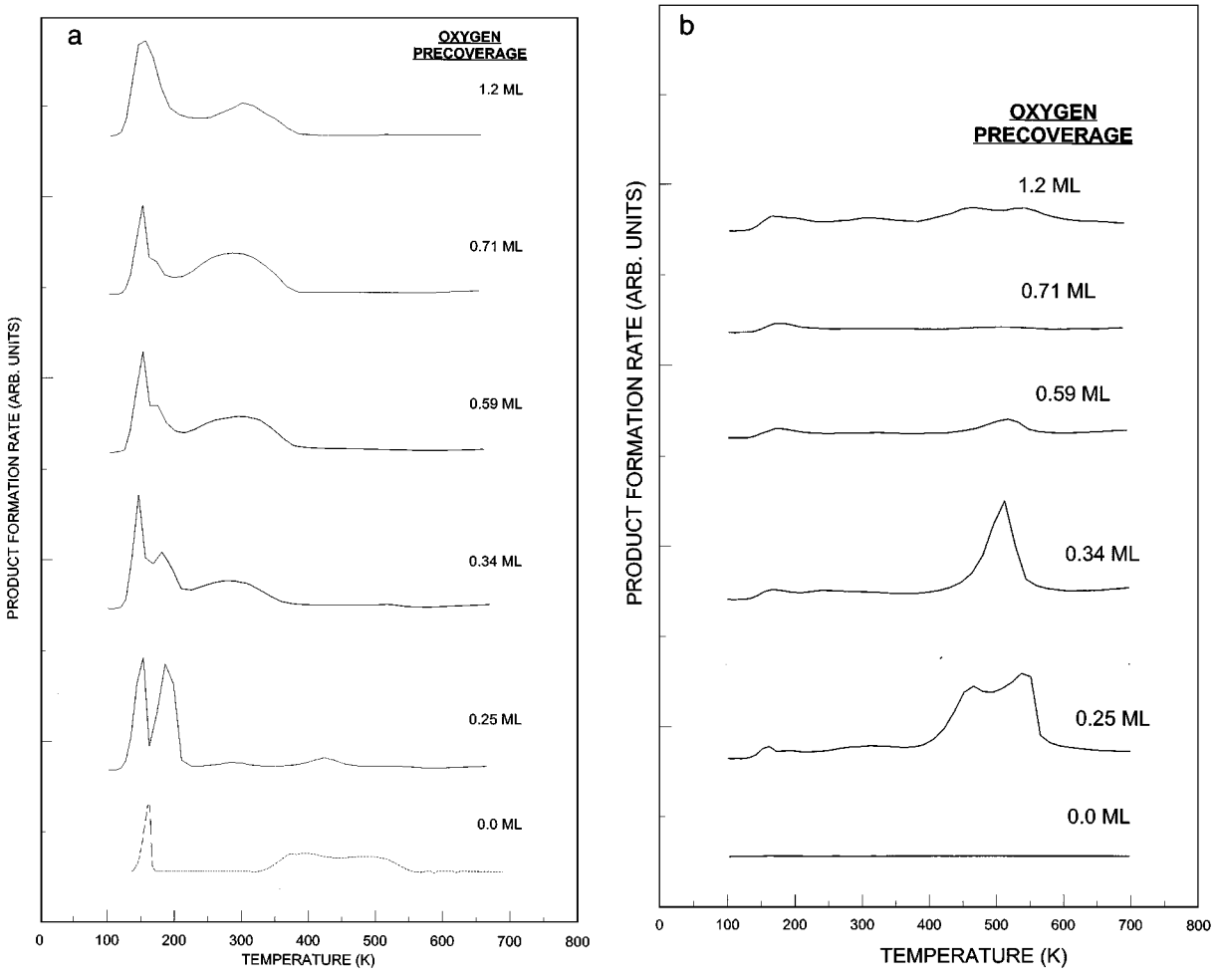

FIG. 7. Product TPRS spectra following benzene adsorbed on Pd(111)-O at varying oxygen precoverages: (a) benzene; (b) H_2O; (c) CO_2.

water and CO are also formed in this temperature range. As the water evolution ceases, a small amount of H_2 evolution begins. A second CO peak appears at 530 K. C(a) remains on the surface after the reaction runs to completion.

DISCUSSION

4.1. Oxygen on Pd(111)

It might be expected that as oxygen coverage increases site blocking would decrease the strength of the benzene-surface bonding and reduce the combustion yields. However, the adsorption of large quantities of oxygen on Pd(111) is not a simple process. Banse and Koel [8] have shown that as oxygen coverage on Pd(111) increases, the character of the oxygen/palladium interaction changes. For oxygen coverages less than 0.51 ML, there is only one type of chemisorbed oxygen. For coverages between 0.51 ML and 0.95 ML there is both chemisorbed surface oxygen and subsurface oxygen; the amount of each depends on the surface temperature. At the dosing temperature used with NO_2 exposure to obtain the higher oxygen coverages (530 K), some oxygen is expected to migrate below the palladium surface. This oxygen will return to the surface and desorb between 750 and 800 K. Further, above a coverage of 0.95 ML oxygen penetrates below the surface and palladium oxide forms at or near the surface. The work of Banse and Koel demonstrates that at the different oxygen coverages employed in this study, the adsorbed hydrocarbons will experience different surface oxygen structures. We believe the unusual evolution of binding states and the maxima in reactivity with oxygen coverage are related to the complex surface structures that form with increasing oxygen coverage. Indeed the distinct changes in reactivity observed between 0.71 and 1.2 ML may originate in oxygen-driven surface reconstructions.

The nature of oxygen/palladium interactions has been studied in greater depth on Pd(110) using STM (24) and XPS (25). It has been found that at oxide coverages exceeding 0.5 ML, a subsurface oxygen state begins to form (25). If oxygen is dosed at high pressures, it exclusively forms a surface oxide layer, which then decomposes upon heating to a

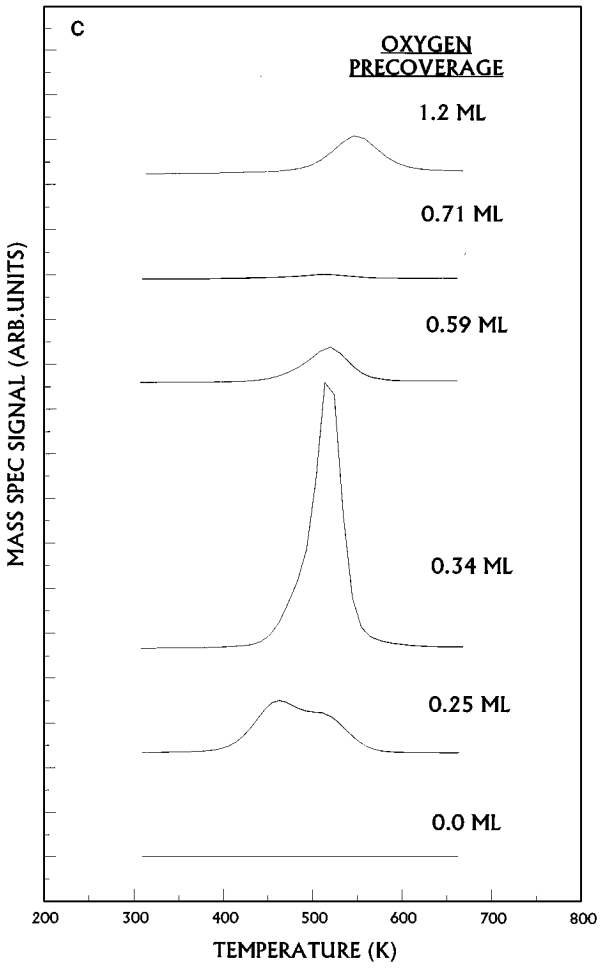

FIG. 7—*Continued*

subsurface oxygen state. Tanaka *et al.* (24) have observed that reconstruction of the Pd(110) surface occurs with oxygen exposure; missing and/or added row structures are created and the distance between the close-packed Pd(110) rows is dependent on oxygen coverage. To date no such studies have been published for the Pd(111) surface.

4.2. Mechanisms of Alkene Combustion

Ethene on O/Pd(111) is much less reactive than the other hydrocarbons studied in this work. The fact this is also true on Pd(100) (10) demonstrates that this low reactivity is not unique to the (111) surface. However, on other metals ethene is not as unreactive. When coadsorbed with 0.23 ML oxygen on Pt(111) ethene adsorbs in both π-bonded and di-σ-bonded configurations (26). On Pt(111) the di-σ configuration reacts in significant quantities to form combustion products, while the π-bonded ethene either desorbs or converts to the reactive di-σ form. In contrast, on Pd(100) an oxygen coverage of 0.25 ML inhibits the di-σ configuration of ethene, thereby suppressing surface reaction (27). Therefore, since there is so little reaction occurring on O/Pd(111), even though it adsorbs readily, we infer that ethene most likely is primarily π-bound and readily desorbs without reaction. Indeed previous studies on Pd(100) suggest also that the absence of a vinylic C-H bond may in ethene be related to its relatively low combustion reactivity.

Since water formation from the recombination of adsorbed H and O reaches a maximum rate in TPRS near 270 K (5), the lower temperature water peaks may arise from the direct attack of ethene by adsorbed oxygen. On the clean surface, ethene dehydrogenation yields two hydrogen desorption features; the first is desorption limited and occurs at 330 K, the second, a reaction-limited peak, is at 420 K. Therefore the broad H_2O peak centered at 290 K could be due to ethene dehydrogenation, followed by oxygen scavenging of the surface hydrogen. Since no H_2O or H_2 peaks occur at or near 420 K, it is apparent that coadsorbed oxygen destabilizes the dehydrogenated fragments, most likely by direct reaction. The identity of the intermediate formed in the release of water near 200 K is unknown. All of the adsorbed ethylene is not partially

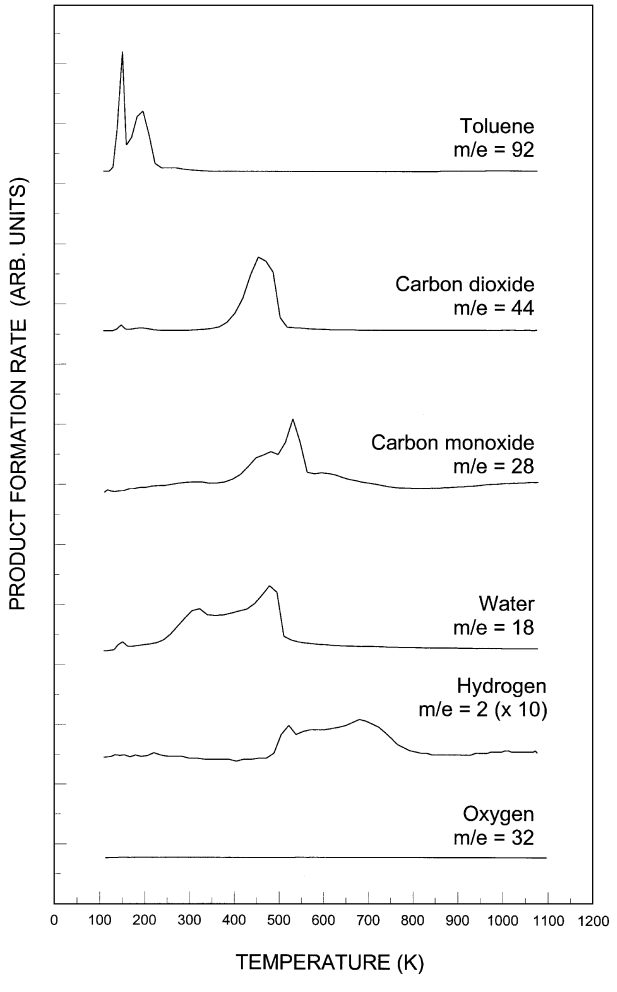

FIG. 8. TPRS spectra of toluene adsorbed on Pd(111)-$p(2 \times 2)$-O.

dehydrogenated to C_2H_3 in the low temperature route exhibited, since stoichiometry would require the ratios of water in the two peaks to be no more than 3 : 1; there is far too little water in the low temperature peak. Rather, it appears that desorption and oxidation of ethylene are competitive over the entire temperature range between 200–400 K.

The patterns of product evolution in the combustion of propene, 1-butene, and 1,3-butadiene on 0.25 ML O/Pd(111) are all nearly identical. Except for a small shift in temperature of the higher temperature water peak at a coverage of 0.25 ML oxygen, the combustion products are evolved at identical temperatures for all three species. The pattern of water formation implies a mechanism whereby the alkene is first partially dehydrogenated (either by Pd or by O(a) attack), and these hydrogens combine with O(a) to yield water. Ignoring the small amount of hydrogen formed from propene oxidation on this surface, we estimate from the relative areas in the two water peaks that two of the six hydrogens are removed in its first reaction to form water. This stoichiometry would appear to rule out an allylic intermediate. This fragment is then attacked by oxygen to produce water, CO_2 and CO simultaneously at 405 K; most of the CO desorbs near 520 K. Some C(a) is left on the surface. As the oxygen is consumed, H_2 evolves. Since hydrogen evolution is a clear indication that the oxygen is consumed by 450 K, the high temperature CO appears to have been formed by attack of the carbon skeleton below this temperature, and the 520 K must be desorption-limited molecular CO.

Unfortunately, in this case we cannot establish by TPRS whether the first reaction (300–400 K) is due to direct attack of the hydrocarbon by adsorbed oxygen or scavenging of hydrogen from already-dehydrogenated hydrocarbon fragments. Water formation from recombination of adsorbed H and O occurs near 270 K (5), which is sufficiently near the temperature of the first water peak in the olefin combustion (not including ethene), consistent with a prior partial dehydrogenation on the $p(2 \times 2)$O surface. The route to water formation at 220 K observed by Davis and Barteau [5] on Pd(111), due to direct transfer of acidic hydrogens from the carboxylic acids to surface oxygen was not observed in the combustion reactions studied here. Thus we can conclude that hydrogen transfer from the alkenes to surface oxygen is not the same for alkenes as for the carboxylic acids. Furthermore, hydrogen evolution from propene dehydrogenation on clean Pd(111) commences near 300 K (20) due to a desorption-limited step and spans the temperature range over which water formation occurs initially.

On clean Pd(111) ethylidyne is formed from ethylene at 300 K, demonstrating that C-H scission does occur by 300 K (28); by analogy one could expect C-H cleavage for propene, etc. to occur at similar temperatures, forming alkylidyne intermediates. However, ethylidyne formation from ethylene on Pd(111) is clearly suppressed by the $p(2 \times 2)$-O structure (although known to occur (29)), since the combustion yield is so low. Furthermore, on Pd(100) the vinylic hydrogen in propene is selectively removed by adsorbed oxygen initially (10, 11). Therefore alkylidyne species are probably not involved in the combustion process.

A few general observations about the effects of increasing coverage can be discussed. For propene, the water production is largest at an oxygen coverage of 0.25 ML and decreases as the coverage is increased. The yields of CO_2 and CO increase to an oxygen coverage of 0.34 ML and then decrease at higher oxygen exposures. Clearly, there is preferential reaction of adsorbed oxygen with hydrogen, rather than carbon, at the lower oxygen coverages. Such behavior would be expected strictly from the activation energies for the recombination reactions (Fig. 1), but the true explanation may be more complex.

Comparison of the amounts of combusted hydrocarbons (Table 2) demonstrates that at saturation coverages on the surfaces covered with 0.25 ML oxygen, propene, 1-butene, and 1,3-butadiene combust to about the same relative extent on Pd(111) and (100), with butadiene being somewhat more reactive. This higher reactivity could originate from a slightly higher binding energy of the diene to the surface, but no significant difference in binding energy is apparent in the desorption behavior of propene and butadiene, for example. One difference between the reactions on the two different surfaces lies in the apparent activation energies for product formation (Table 3). The combustion products generally begin to exhibit lower energies on Pd(100) than on Pd(111). Hence on Pd(100) the first combustion step was attributed to oxygen attack of vinylic hydrogens (10); a similar conclusion cannot be made for the reaction on the (111) surface. However, the general two-step alkene combustion mechanism appears to hold for both Pd(111) and (100); the

TABLE 2

Combustion Product Yields at 0.25 ML O/Pd by Molecule (In ML)

	CO_2	CO	Total HC combusted
Pd(111)			
Ethene	0.0048	0	0.0024
Propene	0.0083	0.038	0.015[a]
1-Butene	0.0048	0.028	0.0083[a]
1,3-Butadiene	0.0042	0.092	0.024[a]
Benzene	0.044	0.046	0.015[a]
Toluene	0.027	0.034	0.0087[a]
Pd(100) [10]			
Ethene	0.04	0	0.020
Propene	0.01	0.03	0.013[a]
1-Butene	0.01	0.04	0.013[a]
1,3-Butadiene	0.03	0.07	0.025[a]

[a] Combustion yield is reaction-limited by surface oxygen.

surface geometry does not seem to play an overriding role in the overall reaction scheme.

4.3. Mechanisms of Aromatic Combustion

A significant difference between the mechanisms of benzene and olefin combustion on 0.25 ML O/Pd(111) is that there is no low activation energy route to water (300 K) for benzene. The simultaneous evolution of water and CO_2, commencing at 400 K and peaking at 450 K, suggests a direct attack of oxygen on adsorbed benzene. At higher oxygen coverages combustion is suppressed.

In contrast to benzene, toluene combusts much like propene. The low temperature water peak is attributable to hydrolysis of the methyl hydrogens on the toluene. This proves that to some extent acidity comparisons can be used to predict relative reactivity on the oxygen-covered surface, at least for the aromatics. This trend was also true for arene combustion on Pd(100) at 0.25 ML O (11). The reactivity of the hydrogens on the ring in toluene is similar to the hydrogens on benzene which would be expected.

Comparison of the combustion product activation energies for saturation coverages of benzene and toluene on the (111) and (100) O/Pd surfaces (Table 3) reveals a few differences. Reaction pathways exhibit activation energies ranging from about 17–40 kcal/mol (excepting the minor pathway for ethylene combustion). Since under steady-state conditions surface carbon must be removed from the surface to maintain catalytic activity, the rate-limiting step in combustion of alkenes and arenes appears to be scavenging of adsorbed carbon or carbonaceous fragments by oxygen. The activation energy characteristic of this process on both Pd(111) and Pd(100) is 30 kcal/mol.

On both surfaces toluene reacts first via the methyl group, followed by the phenyl group. This reaction occurs at a lower temperature on Pd(100). However, benzene combustion occurs at similar temperatures, but on the (111) surface combustion occurs in two separate stages, while on the (100) surface only one pathway was observed.

5. SUMMARY

In this work the interactions of ethene, propene, 1-butene, 1,3-butadiene, benzene, and toluene were studied on Pd(111) at oxygen coverages up to 1.2 ML. Combustion, yielding H_2O, CO_2, and CO, was the only observable reaction. At an oxygen coverage of 0.25 ML propene, butene, and butadiene combust by a two-stage reaction mechanism. Adsorbed oxygen reacts with dehydrogenation fragments, thereby clearing the surface to enable further hydrocarbon decomposition. Although evidence which suggests that

TABLE 3

Estimated Activation Energies (kcal/mol) for Combustion Product Evolution at 0.25 ML O/Pd

	H_2O				CO_2				CO			
Pd(111)												
Ethene	10.0 (175 K)	16.9 (290 K)				26.9 (455 K)						
Propene		17.8 (305 K)	23.6 (400 K)		23.9 (405 K)			23.9 (405 K)		30.9 (520 K)		
1-Butene		17.8 (305 K)	23.0 (390 K)		22.0 (375 K)	27.2 (460 K)		23.0 (390 K)		30.6 (515 K)		
1,3-Butadiene		18.4 (315 K)	22.7 (385 K)		20.5 (350 K)	23.9 (405 K)		22.0 (375 K)		30.9 (520 K)		
Benzene				27.5 (465 K)	31.8 (535 K)	26.9 (455 K)	29.7 (500 K)		26.9 (455 K)	31.2 (525 K)		
Toluene		18.7 (320 K)		28.1 (475 K)		26.9 (455 K)			28.1 (475 K)	31.5 (530 K)	35.5 (595 K)	
Pd(100) (10, 11)												
Ethene			20.7 (340 K)			18.5 (305 K)	33.3 (540 K)					
Propene		16.3 (270 K)	19.4 (320 K)		15.7 (260 K)	19.4 (320 K)	23.2 (380 K)		27.0 (440 K)		35.6 (575 K)	
1-Butene		16.3 (270 K)	19.4 (320 K)		15.7 (260 K)	20.1 (330 K)			27.0 (440 K)		37.2 (600 K)	
1,3-Butadiene			20.7 (340 K)			21.0 (345 K)			27.0 (440 K)		36.9 (595 K)	
Benzene				28.0 (460 K)		28.0 (450 K)					37.0 (600 K)	
Toluene		17.0 (280 K)	25.0 (405 K)			25.0 (410 K)	29.0 (470 K)		29.0 (465 K)		40.0 (640 K)	

oxygen directly attacks partially dehydrogenated hydrocarbon fragments was seen, oxygen-containing intermediates are clearly too reactive on the Pd(111) surface to evolve into the gas phase. Further study is required to define the step by step reaction mechanisms for the combustion process.

REFERENCES

1. Hegedus, L. L., and Gumbleton, J. J., *CHEMTECH*. **10**, 630 (1980).
2. Taylor, K. C., *in* "Catalysis-Science and Technology," (J. R. Anderson and M. Boudart, Eds.), Vol. 5, p. 119. Springer-Verlag, Berlin, 1984.
3. Smidt, J., Hafner, W., Jira, R., Sedlmeier, J., Sieber, R., Ruttinger, R., and Kojer, H., *Angew Chem*. **71**, 176 (1959).
4. Davis, J. L., and Barteau, M. A., *Surf. Sci.* **268**, 11 (1992).
5. Davis, J. L., and Barteau, M. A., *Surf. Sci.* **256**, 50 (1991).
6. Davis, J. L., and Barteau, M. A., *Surf. Sci.* **197**, 123 (1988).
7. Omerod, R. M., and Lambert, R. M., *Catal. Lett.* **6**, 121 (1990).
8. Banse, B. A., and Koel, B. E., *Surf. Sci.* **232**, 275 (1990).
9. Peuckert, M., *J. Phys. Chem*. **89**, 2481 (1985).
10. Guo, X. C., and Madix, R. J., *J. Am. Chem. Soc.* **117**, 5523 (1995).
11. Guo, X. C., and Madix, R. J., *J. Chem. Soc. Faraday Trans.* **91**(20), 3685 (1995).
12. Guo, X., Hoffman, A., and Yates, J. T., *J. Chem. Phys.* **90**, 5787 (1989).
13. Schlatölter, T., and Heiland, W., *Surf. Sci.* **323**, 207 (1995).
14. Odörfer, G., Plummer, E. W., Freund, H.-J., Kuhlenbeck, H., and Neumann, M., *Surf. Sci.* **198**, 331 (1988).
15. Conrad, H., Ertl, G., and Latta, E. E., *Surf. Sci.* **41**, 435 (1974).
16. Conrad, H., Ertl, G., and Küppers, J., *Surf. Sci.* **76**, 323 (1978).
17. Ko, E. I., Ph.D. thesis, Stanford University, 1980.
18. Redhead, P. A., *Vacuum* **12**, 203 (1962).
19. Mass Spectrometry Data Centre, "Eight Peak Index of Mass Spectra," Unwin, Old Working, 1983.
20. Vasquez, N., Jr., Ph.D. thesis, Stanford University, 1997.
21. Davis, J. L., and Barteau, M. A., *Surf. Sci.* **208**, 383 (1989).
22. Hoffmann, H., Zaera, F., Ormerod, R., Lambert, R., Wang, L., and Tysoe, W., *Surf. Sci.* **232**, 259 (1990).
23. Netzer, F. P., and Mack, J. U., *J. Chem. Phys.* **79**, 1017 (1983).
24. Tanaka, H., Yoshinobu, J., and Kawai, M., *Surf. Sci.* **327**, L505 (1995).
25. Bondzie, V. A., Kleban, P., and Dwyer, D. J., *Surf. Sci.* **347**, 319 (1996).
26. Steininger, H., Ibach, H., and Lehwald, S., *Surf. Sci.* **117**, 685 (1982).
27. Stuve, E. M., and Madix, R. J., *Surf. Sci.* **160**, 293 (1985).
28. Gates, J. A., and Kesmodel, L. L., *Surf. Sci.* **124**, 68 (1983).
29. Nascente, P. A. P., Van Hove, M. A., and Somorjai, G. A., *Surf. Sci.* **250**, 167 (1991).
30. Bartmers, J. E., and Mciver, R. T., Jr.,"Gas Phase Ion Chemistry," (M. T. Bowers, Ed.), Vol. 2, p. 87. Academic Press, New York, 1979.